7 The System Function and Measurement System Models

7.1 Direct Measurement of the System Function

In the previous Chapters we have obtained explicit expressions for the transfer functions $t_R(\omega), t_G(\omega)$ that define all the electrical and electro-mechanical components of an ultrasonic measurement system and we gave some examples of simple calibration setups where we can also obtain explicit expressions for the acoustic/elastic transfer function, $t_A(\omega)$. When all these transfer functions are combined with the Thévenin equivalent voltage of the pulser, $V_i(\omega)$, we have a model of the entire ultrasonic measurement system where the output voltage, $V_R(\omega)$, is given by

$$V_R(\omega) = t_G(\omega) t_R(\omega) t_A(\omega) V_i(\omega). \tag{7.1}$$

In section 7.3 we will give some examples of combining all of these models and measurements to synthesize the output voltage of an ultrasonic measurement system. Of course this type of synthesis requires a considerable number of measurements since we must obtain the equivalent voltage and electrical impedance of the pulser, the transfer matrices of the cabling, the impedances (electrical and acoustical) and sensitivities of the transducers, and the electrical impedance and amplification factor of the receiver. However, there is an alternative approach where we combine $t_R(\omega), t_G(\omega)$, and $V_i(\omega)$ into a single factor, $s(\omega)$, called the *system function*, where

$$s(\omega) = t_R(\omega) t_G(\omega) V_i(\omega). \tag{7.2}$$

In terms of the system function Eq. (7.1) reduces to simply:

$$V_R(\omega) = s(\omega) t_A(\omega). \tag{7.3}$$

For any calibration setup where we can model the transfer function $t_A(\omega)$ explicitly and where we measure the frequency components of the received voltage, $V_R(\omega)$, Eq. (7.3) shows that we can obtain the system function by deconvolution, i.e.

$$s(\omega) = \frac{V_R(\omega)}{t_A(\omega)}. \tag{7.4}$$

In practice, to reduce the sensitivity of the deconvolution to noise, we use a Wiener filter (see Appendix C) and obtain the system function from

$$s(\omega) = \frac{V_R(\omega) t_A^*(\omega)}{|t_A(\omega)|^2 + \varepsilon^2 \max\left\{|t_A(\omega)|^2\right\}}, \tag{7.5}$$

where ε is a constant that is used to represent the noise level present and $(\ )^*$ indicates the complex-conjugate.

The system function contains all the electrical and electromechanical components of the ultrasonic measurement system, so with one measurement of $V_R(\omega)$ in a well characterized calibration experiment, Eq. (7.5) allows us to characterize the effects of all those components at once. This is obviously a very convenient alternative to having to measure all the elements that make up $s(\omega)$. This method of determining the system function is done at a fixed set of system settings (e.g. energy and damping settings on a spike pulser, gain settings on the receiver) and with a given set of cables and transducers. If another experiment such as a flaw measurement is performed at exactly the same settings and with the same components the system function obtained from the calibration setup will be the same as for the flaw measurement. This fact allows us to quantitatively determine the effects that all the electrical and electromechanical parts of the measurement system have on a flaw measurement. Since $s(\omega)$ has nothing to do with the response of a flaw being measured, it is important to be able to characterize (and eliminate) those parts of the measured signals that are not flaw dependent so that we can determine a response more directly related to the flaw being examined.

Another way that we can use knowledge of $s(\omega)$ is to combine it with beam propagation and flaw scattering models that can model the

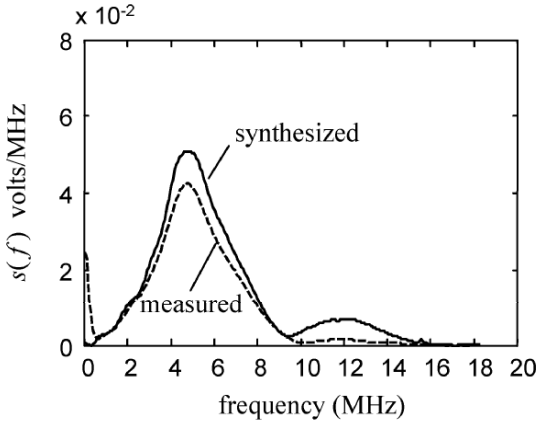

Fig. 7.1. A system function, $s(f)$, measured directly by deconvolution (dashed line) or synthesized by measuring all the electrical and electromechanical components contained in $s(f)$ (solid line).

acoustic/elastic transfer function, $t_A(\omega)$ explicitly. In later Chapters we will show just how to develop such detailed models. By combining a modeled $t_A(\omega)$ and a measured $s(\omega)$, Eq. (7.3) shows that we can predict the actual measured voltage, $V_R(\omega)$, in a flaw measurement setup in an absolute sense. This capability gives us a powerful engineering simulation tool to design and evaluate ultrasonic NDE inspections.

In using a directly measured system function, one must re-measure that function whenever a system setting or system component is changed and this approach does not permit us to determine the significance of individual changes, such as a replacement of a transducer, for example, without such a re-measurement. Determining $s(\omega)$ by combining a knowledge of $V_i(\omega)$ and all the components that make up $t_R(\omega)$ and $t_G(\omega)$, however, does allow us to examine the effects of such changes. Of course, either a directly measured system transfer function or one synthesized from its components should agree with each other. This is the case, as illustrated in Fig. 7.1, where a system function was both directly measured by deconvolution and constructed from individual measurements of all the electrical and electromechanical components [7.1].

7.2 System Efficiency Factor

In [Fundamentals] a quantity which is closely related to the system function was defined called the *system efficiency factor*, $\beta(\omega)$. This system efficiency factor is related to the measured voltage, $V_R(\omega)$, as follows:

$$V_R(\omega) = \beta(\omega)\frac{p_{ave}(\omega)}{\rho c v_0(\omega)}, \tag{7.6}$$

where $p_{ave}(\omega)$ is the average pressure generated by the incident waves at the receiving transducer, $v_0(\omega)$ is the output velocity of the transmitting transducer (which is assumed to act as a piston) and ρc is the specific acoustic impedance of the material into which the transmitting transducer radiates. The blocked force $F_B(\omega) = 2p_{ave}(\omega)S_R$, where S_R is the area of the receiving transducer, and the force transmitted by the sending transducer $F_t(\omega) = Z_r^{T;a}(\omega)v_0(\omega) = \rho c S_T v_0(\omega)$ for a piston transducer at high frequencies, where S_T is the area of the transmitting transducer. Thus, combining these relations with the two equivalent forms

$$V_R(\omega) = s(\omega)\frac{F_B(\omega)}{F_t(\omega)} = \beta(\omega)\frac{p_{ave}(\omega)}{\rho c v_0(\omega)} \tag{7.7}$$

we see that the system function and the system efficiency factor are just proportional to one another, where

$$s(\omega) = \frac{S_T}{2S_R}\beta(\omega), \tag{7.8}$$

so it makes no difference if we characterize our measurement system with either of these quantities.

In determining the system function or system efficiency factor experimentally by deconvolution in a reference experiment, the values of $s(\omega)$ or $\beta(\omega)$ should not depend on the choice of that reference experiment and it's corresponding transfer function, $t_A(\omega)$. Schmerr et al. [7.2] demonstrated this fact by using a number of different reference setups to calculate the system efficiency factor. Some of the simple calibration setups where the transfer function $t_A(\omega)$ is known are shown in Fig. 7.2.

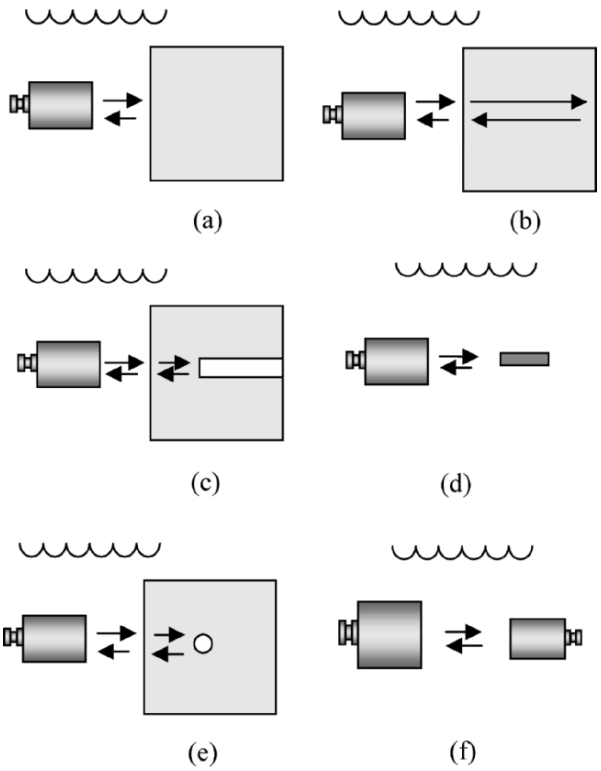

Fig. 7.2. Reference experiments that can be used to determine the system function or system efficiency factor where circular planar transducers are involved: **(a)** reflection from a plane front surface of a block at normal incidence, **(b)** reflection from the back surface of a block at normal incidence, **(c)** reflection from an on-axis flat-bottom hole at normal incidence, **(d)** reflection from an on-axis solid cylinder at normal incidence, **(e)** reflection from an on-axis side-drilled hole at normal incidence, and **(f)** two transducers (not necessarily the same) whose axes are aligned.

Cases (a) and (f) were discussed in Chapter 5. Cases (b), (c), (d) and (e) can be found in [7.2] and [Fundamentals]. All the cases shown in Fig. 7.2 are suitable for determining the system function for circular, planar transducers in pulse-echo immersion setups except Fig. 7.2 (f) which can be used for circular, planar transducers in immersion pitch-catch setups. In Chapter 8 we will develop an explicit expression for $t_A(\omega)$ in the setup shown in Fig. 7.2 (a) for a circular, spherically focused transducer that can be used to determine $s(\omega)$ for that type of transducer

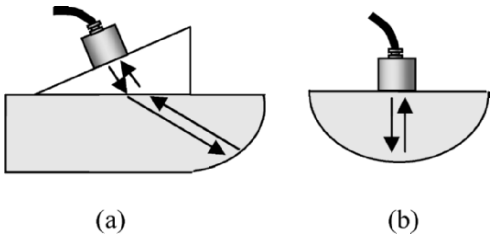

Fig. 7.3. Reference experiments that can be used to determine the system function for **(a)** an angle beam probe test setup where the waves are reflected from the curved surface of a calibration block, and **(b)**, a contact setup where the waves are reflected from a curved surface of a block.

as well as transfer functions for planar rectangular transducers and cylindrically focused rectangular transducers. In Chapter 13 we will show how a multi-Gaussian beam model can be used to numerically determine the transfer function $t_A(\omega)$ for the pulse-echo contact angle beam shear wave setup of Fig. 7.3 (a) where the waves are reflected from the cylindrical interface of a standard calibration block. That same approach can also be used for other contact testing setups such as the one shown in Fig. 7.3 (b) or in other contact setups with planar or curved surfaces. In contact problems, however, one must be aware of the fact that changes of the thin fluid couplant layer between the transducer and the component being inspected (or between the transducer wedge and the component) and non-uniform component surface conditions can produce measured response variabilities that must be carefully considered.

7.3 Complete Measurement System Modeling

The ultimate test of the ability of all these models and measurements to simulate an ultrasonic measurement system is to compare the measured output voltage of a particular setup with one that is synthesized from the models/measurements we have discussed in previous Chapters. Consider, for example, a calibration setup of the type shown in Fig. 7.2 (f) where two planar transducers of the same nominal radius are placed opposite to each other in an immersion tank with their axes aligned. An explicit acoustic/elastic transfer function for this configuration was given in Eq. (5.12) for an ideal lossless fluid. Adding attenuation into this ideal model as shown in Chapter 5 (see Eq. (5.22a)) we have a complete

acoustic/elastic transfer function for this example. Combining this transfer function with a measured system function gives the frequency components of the measured output voltage (Eq. (7.3)). Finally, taking an inverse Fourier transform out this output voltage spectrum then yields a time domain A-scan signal for the entire system. We can simulate this A-scan signal using a system function that is calculated from Eq. (7.2), using measurements of all the components that make up $t_G(\omega)$ and $t_R(\omega)$ together with $V_i(\omega)$. Recall, these transfer functions were given by

$$t_R(\omega) = \frac{K Z_o^e S_{vI}^B}{\left(Z_{in}^{B;e} R_{11} + R_{12}\right) + \left(Z_{in}^{B;e} R_{21} + R_{22}\right) Z_o^e} \tag{7.9}$$

and

$$t_G(\omega) = \frac{Z_r^{A;a} S_{vI}^A}{\left(Z_{in}^{A;e} T_{11} + T_{12}\right) + \left(Z_{in}^{A;e} T_{21} + T_{22}\right) Z_i^e}. \tag{7.10}$$

The pulser used here was a Panametrics 5052 PR pulser/receiver operating at an energy setting of 1 and a damping setting of 7. The open-circuit voltage of the pulser was measured to obtain $V_i(\omega)$ and the pulser impedance, $Z_i^e(\omega)$,was measured by placing a 50 ohm resistor across the pulser output and measuring the resulting voltage across this resistance, as outlined in Chapter 2. The transfer matrix components, $[T_{11}, T_{12}, T_{21}, T_{22}]$ of the cabling between the pulser and transmitting transducer *A* and the cable components, $[R_{11}, R_{12}, R_{21}, R_{22}]$ for the cabling between the receiving transducer *B* and the receiver were both measured as functions of frequency using different cabling termination conditions as discussed in Chapter 3. The receiver gain, $K(\omega)$, and impedance, $Z_0^e(\omega)$, were obtained from measurements of voltage and current at the receiver inputs and outputs, as described in Chapter 5, at receiver gain and attenuation settings of 20 dB and 12 dB, respectively, and with the filter control of the receiver set to "off". The two transducers used in this pitch-catch setup were two nominally identical 5 MHz, 6.35 mm diameter planar transducers. Their electrical impedances, $Z_{in}^{A;e}(\omega)$ and $Z_{in}^{B;e}(\omega)$, and their sensitivities, S_{vI}^A and S_{vI}^B, were found using the electrical measurements which were discussed in Chapter 6. Finally, the acoustic radiation impedance of the transmitting transducer *A*, $Z_r^{A;a}(\omega)$, which appears in the sound generation transfer function, was computed from the high frequency

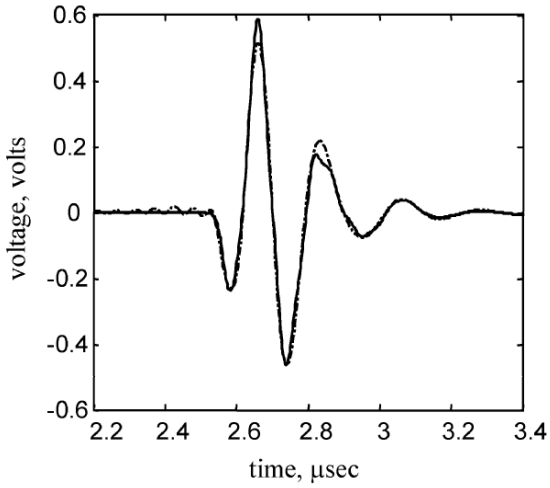

Fig. 7.4. Directly measured output voltage signal of an ultrasonic pitch-catch measurement system (solid line) and the voltage synthesized by measurement and modeling of all the ultrasonic components (dashed-dotted line) for a pair of 5 MHz, 6.35 mm diameter planar transducers in the configuration of Fig. 7.2 (f).

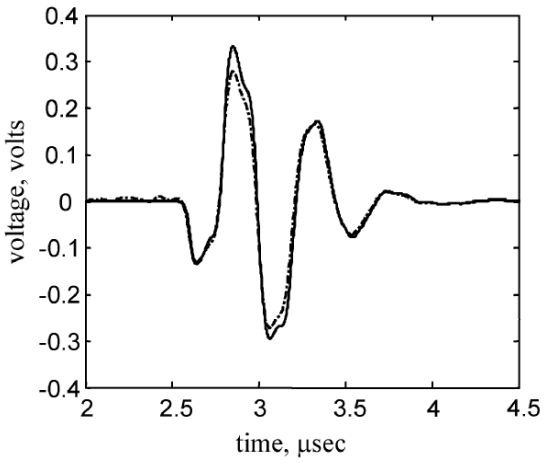

Fig. 7.5. Directly measured output voltage signal of an ultrasonic pitch-catch measurement system (solid line) and the voltage synthesized by measurement and modeling of all the ultrasonic components (dashed-dotted line) for a pair of 2.25 MHz, 12.7 mm diameter planar transducers in the configuration of Fig. 7.2 (f).

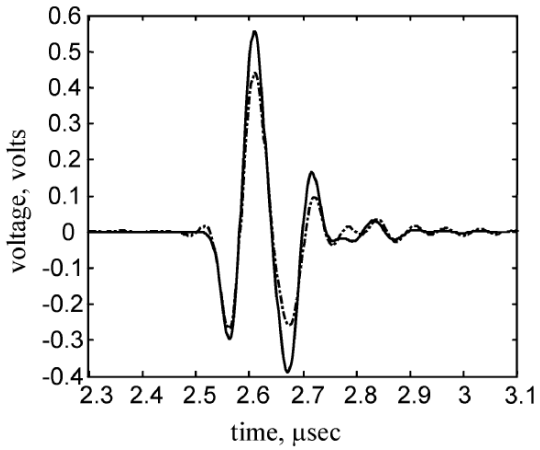

Fig. 7.6. Directly measured output voltage signal of an ultrasonic pitch-catch measurement system (solid line) and the voltage synthesized by measurement and modeling of all the ultrasonic components (dashed-dotted line) for a pair of 10 MHz, 6.35 mm diameter planar transducers in the configuration of Fig. 7.2 (f).

limit expression for a piston transducer, $Z_r^{A;a} = \rho c S_A$, using the density, $\rho = 1$ gm/cm^3, and measured wave speed, $c = 1481$ m/sec, of the water and a transducer area, $S_A = \pi a^2$, calculated from the nominal radius of the transducer, $a = 3.175$ mm. The distance, *D*, between the two transducers was set at $D = 67$ mm and the attenuation of the water (at room temperature) was taken as the value given by Eq. (5.21). Figure 7.4 shows a comparison of the directly measured output voltage for this configuration with the voltage synthesized from the measurement and modeling of all the system components. Figure 7.5 shows the corresponding results when a pair of 2.25 MHz, 12.7 mm diameter planar transducers were used instead in the same setup and Fig. 7.6 shows the results for a pair of 10 MHz, 6.35 mm diameter planar transducers. For the 5 MHz transducers a difference of -0.7 dB was observed between the peak-to-peak voltage response of the synthesized signal to that of the measured signal. The predicted waveform using 2.25 MHz transducers shows a difference of −1.1 dB in the peak-to-peak voltage with respect to that of the corresponding measured output voltage. For the 10 MHz transducers a somewhat larger difference (−2.5 dB) was observed. In all cases the predicted waveforms had very similar shapes to the measured ones.

Figure 7.7 shows some similar comparisons between a synthesized signal and a measured signal for the pulse-echo setup shown in Fig. 7.2 (a)

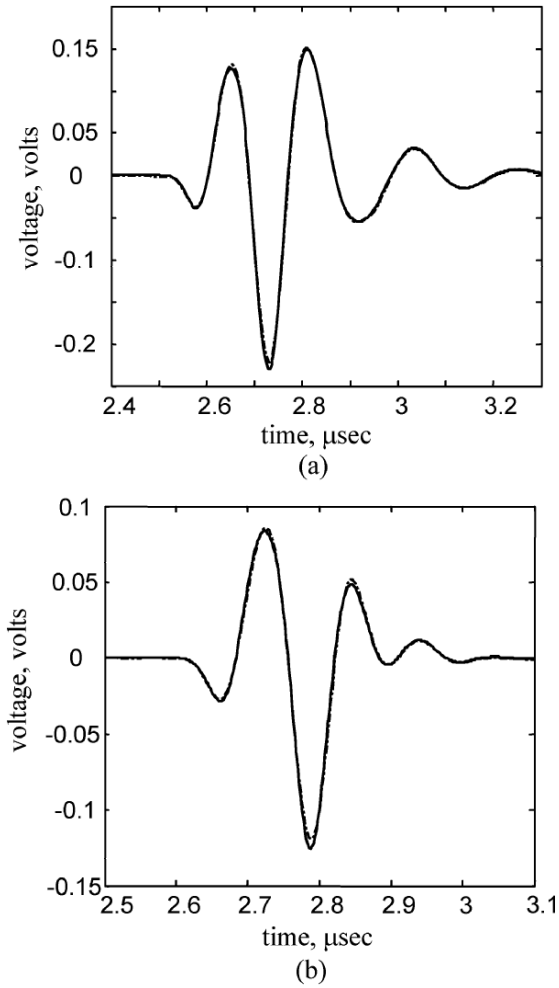

Fig. 7.7. Directly measured output voltage signal of an ultrasonic pulse-echo measurement system (solid line) and the voltage synthesized by measurement and modeling of all the ultrasonic components (dashed-dotted line) for **(a)** a 5 MHz, 6.35 mm diameter planar transducer in the configuration of Fig. 7.2 (a) ,and **(b)** a 10 MHz, 6.35 mm diameter planar transducer in the configuration of Fig. 7.2 (a).

where a planar transducer is receiving the signals reflected from the planar front surface of a solid. The acoustic/elastic transfer function is also available for this configuration (see Eq. (5.16)) in an explicit form. In this case a UTEX 320 square wave pulser/receiver was used in the measurements and

again we compared the received measured signals with a voltage synthesized by combining the acoustic/elastic transfer function, the measured Thévenin equivalent source voltage of the pulser, and the sound generation and reception transfer functions obtained by measuring all the components contained in those functions. Figure 7.7 (a) shows a comparison of the measured and synthesized received voltage when a 5 MHz planar transducer was used in this setup. Figure 7.7 (b) shows the corresponding comparison for a 10 MHz transducer. In both cases the peak-to-peak values of the measured signals agreed with the synthesized wave forms to within about 0.2 dB.

7.4 References

7.1 Dang CJ, Schmerr LW, Sedov A (2002) Modeling and measuring all the elements of an ultrasonic nondestructive evaluation system. II: Model-based measurements. Research in Nondestructive Evaluation 14: 177-201

7.2 Schmerr LW, Song SJ, Zhang H (1994) Model-based calibration of ultrasonic system responses for quantitative measurements. In: Green RE Jr., Kozaczek KJ, Ruud CO (eds) Nondestructive characterization of materials, VI. Plenum Press, New York, NY, pp 111-118

7.5 Exercises

1. The beam of a planar immersion transducer is reflected off the front surface of a steel block (see Fig. 7.2 (a)) and this reference signal can be used to determine the system function. The file FBH_ref contains a sampled reference signal of this type and its corresponding sampled times. Place this file in your current MATLAB directory and then load it with the MATLAB command

```
>> load( ‘ FBH_ref ' )
```

This command will place in the MATLAB workspace 1000 sampled time values in the variable t_ref, and a 1000 point reference time domain waveform in the variable ref. Plot this waveform. Take the FFT of this reference waveform and keep only the first 200 values of the resulting 1000 point spectrum (from 0 to 20 MHz) in a variable, Vc. Plot the magnitude of Vc from 0 to 20 MHz. Use Vc and the data given below to determine the system function via deconvolution (using a Wiener filter) and plot the magnitude of this system function versus frequency from zero

to 20 MHz. Compare this system function with Vc. Use the acoustic/elastic transfer function for this configuration as:

$$t_A = 2R_{12}\exp\left(-2\alpha_{p1}D\right)\left[1-\exp\left(ik_{p1}a^2/2D\right)\right.$$
$$\left.\cdot\left\{J_0\left(k_{p1}a^2/2D\right)-iJ_1\left(k_{p1}a^2/2D\right)\right\}\right]$$

where we have dropped the phase term $\exp\left(2ik_pD\right)$ as it only produces a time delay and the plane wave reflection coefficient is:

$$R_{12}=\frac{\rho_2 c_{p2}-\rho_1 c_{p1}}{\rho_2 c_{p2}+\rho_1 c_{p1}}$$

The parameters for this setup are:

$\rho_1 = 1.0$, $\rho_2 = 7.86$: density of the water and steel, respectively (gm/cm^3)
$c_{p1} = 1484$, $c_{p2} = 5940$: P-wave speeds of the water and steel, respectively (m/sec)
$\alpha_{p1} = 24.79\times10^{-6} f^2$: water attenuation (Np/ mm) with f the frequency (in MHz)
$D = 50.8$: distance from the transducer to the block (mm)
$a = 6.35$: radius of the transducer (mm)
$e = 0.3$: noise coefficient for the Wiener filter

Note that the Bessel functions are available directly in MATLAB. The Bessel function of order zero, $J_0\left(x\right)$, is given by the MATLAB function besselj(0, x) and the Bessel function of order one, $J_1\left(x\right)$, is given by the MATLAB function besselj(1, x).